RESEARCHERID
THOMSON REUTERS

[*Altıntaş* et al.*, 6(12): December, 2017]
IC™ Value: 3.00

ISSN: 2277-9655
Impact Factor: 4.116
CODEN: IJESS7

IJESRT

INTERNATIONAL JOURNAL OF ENGINEERING SCIENCES & RESEARCH TECHNOLOGY

SENSORED VECTOR CONTROL THREE PHASE MOTOR DRIVER DESIGN BASED ON CORTEX M7 ARM

Mert Altıntaş[*1]
[*] Electrical and Electronic Engineering, Ege University, TURKEY

DOI: 10.5281/zenodo.1116696

ABSTRACT

Three-phase brushless motors are an indispensable part of the industry. A significant portion of electricity consumption is the energy consumed by industrial motors. Therefore, these electric motors need to be used efficiently. If these motors are not driven by the suitable inverter, they cannot handle the load or increase losses in the energy. In addition, the system can be inefficient. Since these motors have a high starting torque and controlling rotation speed is difficult, a better control method is preferred rather than a V/f control.

This research aims to control using PMSM (permanent synchronous motor) FOC method and Space vector PWM with the position sensor, which is incremental encoder and. FOC approach, will minimize energy losses. Also, Space vector PWM method reduces the harmonic of the motor current. The FOC approach is to direct the stator rotating field most efficiently using the motor's rotor position information. The incremental encoder will provide the information rotor position and speed. The software structure is achieved through the utilization of a STM32F745VE that is new series Cortex™-M7 32 bit ARM® processor. FOC calculation takes 14.5 microseconds thanks to the Cortex M7 architecture and floating point unit.

KEYWORDS: Synchronous motor, FOC Control of PMSM, ARM, Space Vector Modulation

I. INTRODUCTION

Nowadays, robotic applications grow rapidly and this speeds up the motor position control applications. In this kind of applications, best performance belongs to the PMSM (Permanent Magnet Synchronous Motor). Especially, in the magnets mounted to the surface synchronous motors, ripple torque is quite low because of that L_d and L_q equal to each other. Therefore, it is preferred in torque controlled servo applications very often.

In the high performance PMSM driver designs, some field oriented controlled application using FOC method with encoder feedback FPGA and DSP processors is used together[1 and 2]. With evolving FPGA technologies, there are applications that only include an FPGA chip [3-9].

Besides that, fixed point design applications is made by using C programming language in the PMSM vector applications which used DSP processors belongs to Texas microcontroller family mostly[10 - 17]. In the other hand, similar applications is made by using other companies DSP processor products like MC56F8357 [18] and 56807 [19]. Also, except that DSP processors, there are similar applications like sinus switching [20] applications are made by using 16-bit microcontrollers. In recent years, ARM based Hercules RM46 processor [21] and STM32F407-168MHz ARM microprocessor [22] is used for developing sensored PMSM vector control applications in the literature.

In this study, sensored field oriented controlling is performed for synchronous motor which magnets mounted on the surface by using STM32f745VE-216MHz chip which has Cortex M7 core and 462 MIPS. A 1024 ppr (pulse per revolution) incremental encoder is used for measuring the rotor position.

II. MATERIALS AND METHODS

A. Synchronous Motor Mathematical Model

Permanent magnet synchronous motors (PMSM); is divided into two, surface permanent magnet (SPM) and interior permanent magnet (IPM). SPM motors is much more stable than IPM at torque ripple. At the same time, inductance creates small changes at rotor and stator is quite small according to rotor angle because of that rotor and stator air gap is equal each other in space. For this reason, it is negligible. However, if the IPM

ISSN: 2277-9655
Impact Factor: 4.116
CODEN: IJESS7

synchronous motor driver is designed which has the capabilities for controlling the torque ripple; they are much more successful than the SPM at torque generation.
Motor's voltage, flux and generated torque at d and q axes are given in equation 1-5;

$$V_{qs} = R_s\, i_{qs} + \frac{d\varphi_{qs}}{dt} + \omega\, \varphi_{ds} \qquad (1)$$

$$V_{ds} = R_s\, i_{ds} + \frac{d\varphi_{ds}}{dt} - \omega\, \varphi_{qs} \qquad (2)$$

$$\varphi_{qs} = L_{ds}\, i_{ds} + \varphi_{mag} \qquad (3)$$

$$\varphi_{qs} = L_{qs}\, i_{qs} \qquad (4)$$

$$T_e = \frac{3}{2} p[\varphi_{mag}\, I_{qs} - L_{ds}(1-\xi) I_{ds} I_{qs}] \qquad (5)$$

L_q and L_d inductance are equal because of that d and q axes flux paths are equal at SPM synchronous motors. Thanks to the equality of inductance, at equation 6, ξ is equal to 1. In this way, the torque equation in equation 5 is simplified the torque equation in equation 7. In here, φ_{mag} value is constant, and torque depends only the I_{qs} changes.

$$\xi = L_{qs}/L_{ds} \qquad (6)$$

$$T_e = \frac{3}{2} p[\varphi_{mag}\, I_{qs}] \qquad (7)$$

B. Field Oriented Control

The reason of using field control method for driving synchronous motor is capability of setting the motor's speed and torque. This control method needs motor's two phase currents and rotor position.

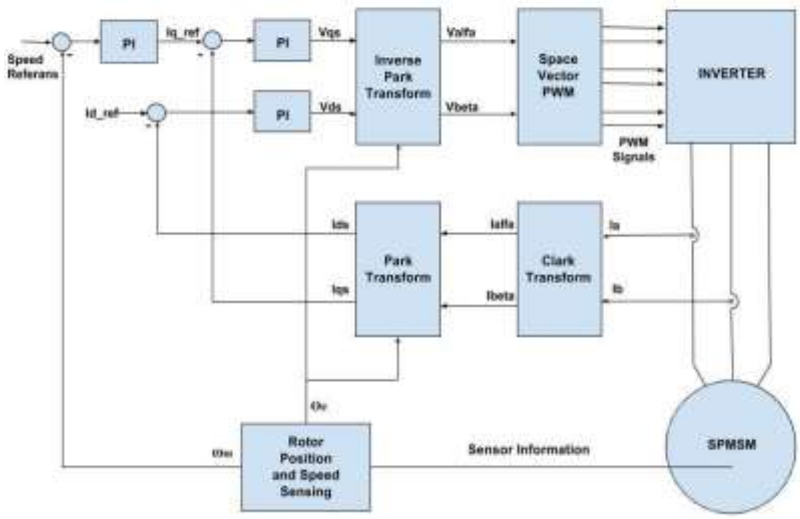

Figure 1 FOC block diagram

As shown Figure 1, currents are controlled in DC domain with PI by using clark and park methods. Then, d-q voltages are calculated by inverse park. With space vector modulation, pulse width modulation periods are calculated to generate desired voltages. Pulse width modulation periods that mentioned before is applied to motor's phases according space vector calculation.

C. Clark and Park Transform

Purpose of the Clark Transformation; defining 120 degree differentiated a, b and c phase currents in 90 degree differentiated alpha-beta axes. As a result of this transformation, three phases current are transformed to the two phases current called alpha and beta. In this way, number of equations is reduced in the system. Clark transformation is performed by 8-10 equations.

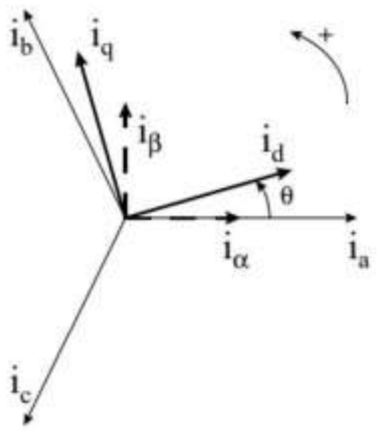

Figure 2 Clark and Park Transform [10]

$$i_{s\alpha} = i_a \quad (8)$$

$$i_{s\beta} = \frac{1}{\sqrt{3}}\, i_a + \frac{2}{\sqrt{3}}\, i_b \quad (9)$$

$$i_a + i_b + i_c = 0 \quad (10)$$

Park transform; if alpha and beta axes which perpendicular is even constant in space, current values change depending on time. By the way of Park transform, alpha and beta axes are rotated up to Θ_e. Because of that resultant of currents depend to Θ_e angle, d-q axes current set is constant. Thus, vector control is provided over these currents. This new axes set is called d-q axes. Park transformation is applied by 11 and 12 equations for alpha and beta currents.

$$i_{sd} = i_{s\alpha} \cos(\theta_e) + i_{s\beta} \sin(\theta_e) \quad (11)$$

$$i_{sq} = -i_{s\alpha} \sin(\theta_e) + i_{s\beta} \cos(\theta_e) \quad (12)$$

D. Inverse Park Transform

By using this transformation, a d-q voltage, which is perpendicular to each other, is transformed to alpha-beta axes for calculating space vector. Inverse Park transformation is calculated by using 13 and 14 equations.

$$V_{s\alpha} = V_{sd} \cos(\theta_e) - V_{sq} \sin(\theta_e) \quad (13)$$

$$V_{s\beta} = V_{sd} \sin(\theta_e) + V_{sq} \cos(\theta_e) \quad (14)$$

E. Space Vector Modulation

Space vector pulse width modulation is a mathematical calculation for determining the inverter's generated V_a, V_b ve V_c phase voltages. T_1, T_2, T_0 values are calculated by equation 15-17.

$$T_1 = \frac{\sqrt{3}\,\mathrm{T_s}\,\mathrm{V_{ref}}}{\mathrm{V_d}} \sin\left(\frac{\pi}{3} - \theta_e\right) \quad (15)$$

$$T_2 = \frac{\sqrt{3}\,\mathrm{T_s}\,\mathrm{V_{ref}}}{\mathrm{V_d}} \sin(\theta_e) \quad (16)$$

$$T_0 = \mathrm{T_s} - \mathrm{T_a} - \mathrm{T_b} \quad (17)$$

According to desired to create vector located in Figure 3, applied T_1, T_2 and T_0 values are determined. In this way, pulse width modulation duty cycle of each phase is determined.

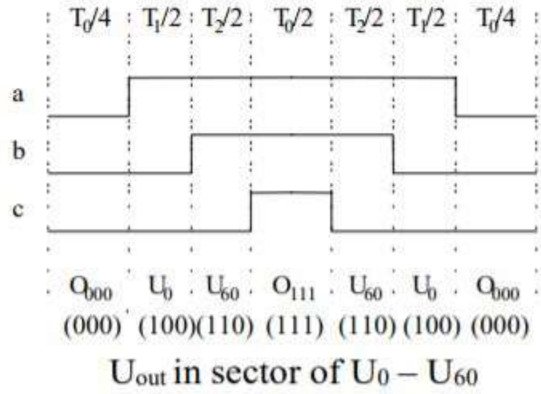

Figure 3 Pulse width modulation duty cycles at Sector 1 [17]

Generated PWM, vectors placed (symmetrically) so they are aligned in the center. In this way, by providing symmetry voltage and current harmonics are reduced. At the same time, since the number of switching is reduced, the switching losses kept at minimum value.

F. Algorithm

Timer1 period is 62.5 µsn (16kHz), Timer2 period is 1msn (1kHz), ADC interrupt is set for depending on Timer1 and sampling in the middle of PWM period. PWM output's works depends on Timer. In Figure 4 shows the algorithm flow diagram.

When the system starts, incremental encoder can't determine the rotor position. At first, a vector must be applied to the stator windings with a constant angle during one second for determine the rotor position, after that rotor is locked to this vector. In this way rotor position is forced a known vector. System runs after this locked position value is accepted for initial angle value.

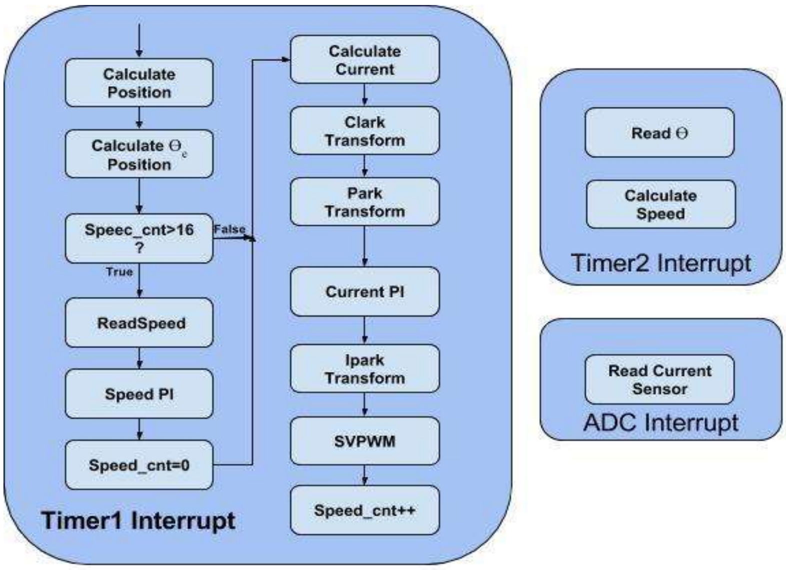

Figure 4 Algorithm flow schematics

III. RESULTS AND DISCUSSION

In Figure 5, Foucault brake is located at the right. Torque that generated by Foucault brake can be controlled by a variable DC power source. At the left, SPM synchronous motor, which has brand name Femsan, is located. Desired value in the oscilloscope is provided by two DAC outputs located in the processor. Measured value on oscilloscope transferred to the computer.

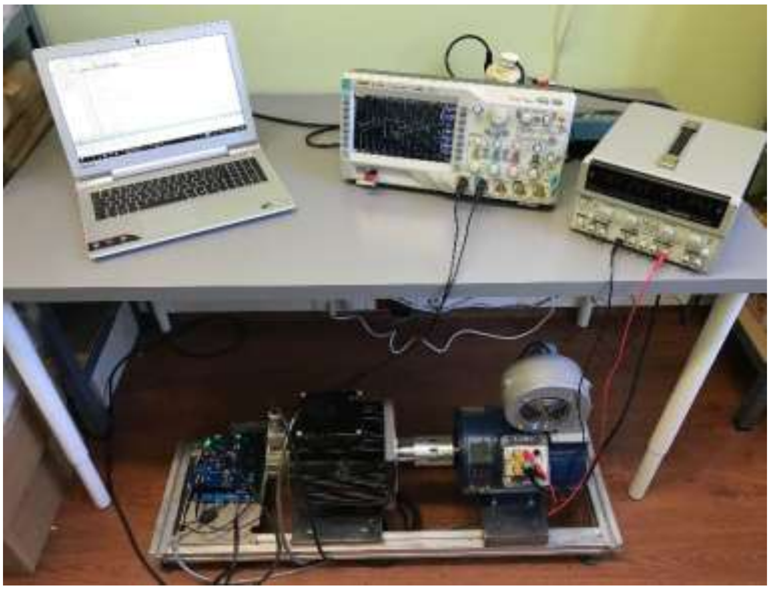

Figure 5 Experimental system

All test results are collected when the speed reference applied to system similar to the Figure 6. When the system is loaded and not loaded, comparative motor speed variations to the speed reference can be seen at Figure 6 and 7. At the No-load system, overshoot occurs at 500 rpm output point. In the loaded system at Figure 7, overshoot occurs relatively small. According to these results, it is seen that the performance of the system to follow the speed reference is better than low speed at high speeds.

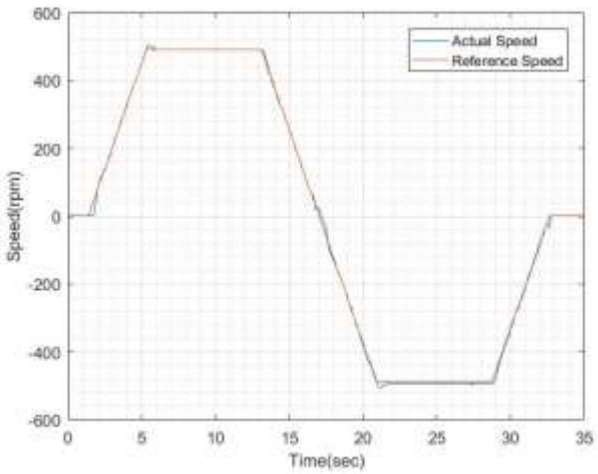

Figure 6 Speed and speed reference when the system is not loaded.

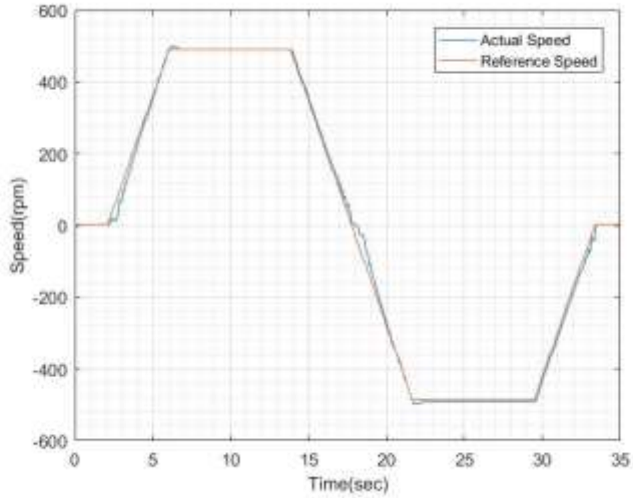

Figure 7 Speed and speed reference at full-load

Measured I_{qs} and I_{ds} currents is shown in Figure 8. Since the field weakening is not used within the rated speed because the permanent magnet synchronous motor, the Id current reference is set to zero. In the Figure 8, blue signal is referred to the measured Id current. This current value is around zero. Orange signal is referred to the I_q current. As shown at the equation 7, at the permanent magnet synchronous motor, I_q current controls the torque directly. While motor is tended to speed up, moment of inertia affect the I_q current curve parabolically.

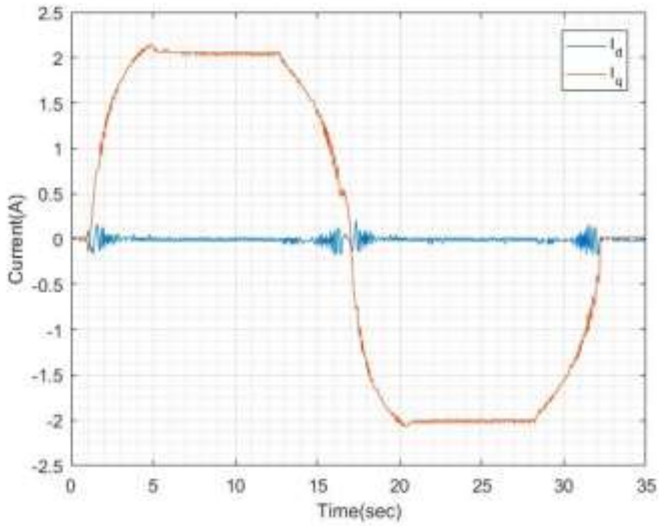

Figure 8 I_q and I_d current at full-load.

ISSN: 2277-9655
Impact Factor: 4.116
CODEN: IJESS7

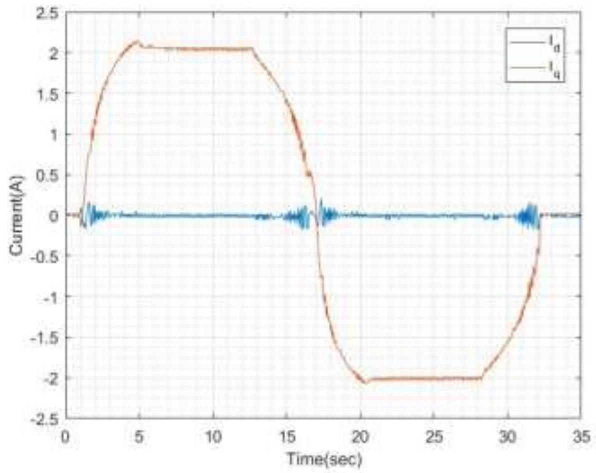

Figure 9 Speed and I_q current at full-load

At the test which is shown at Figure 10, when the system is not loaded, full-load is activated in 9.5 second and Iq current generated in the system and measured speed is shown in the Figure 10. In a sudden changing load system, in the 0.5-second time interval, 20% of speed decrease is observed.

In the same way, when the system is operating at full load, load is driving in 25.5 second. In the 0.5-second time interval, 10% of speed increase is observed.

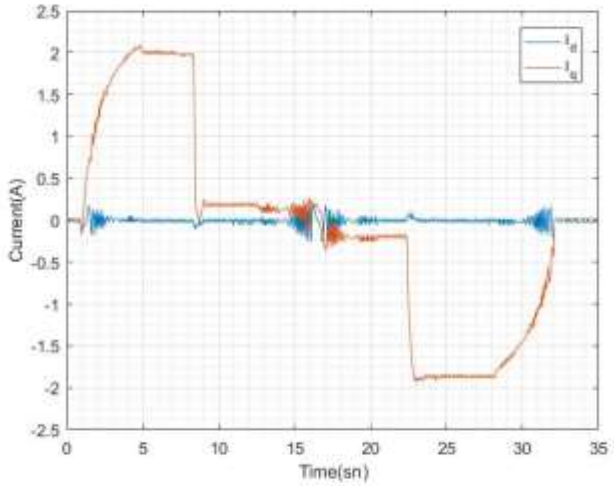

Figure 10 Speed and I_q current when deactivated and activated instantaneously at full-load

At the Figure 11, Foucault brake at the system cause continuous changes at the torque. In such a case, I_q signal which is measured by I_q reference signal which is generated by the system is analyzed. As is seen, measured signal can follow reference signal. At the point of contra flexure or drop-off regions, measured signal is remained behind the system.

Drawing graphics in Figure 11 is exported as an image from Figure 12.

ISSN: 2277-9655
Impact Factor: 4.116
CODEN: IJESS7

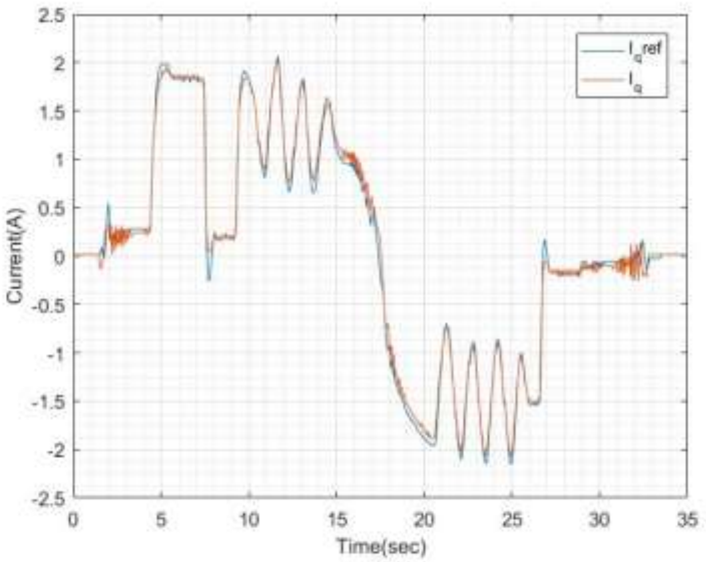

***Figure 11** I_{q}_ref and I_q current when changing load*

***Figure 12** Oscilloscope images of I_{q_ref} and I_q currents at the system's load changes.*

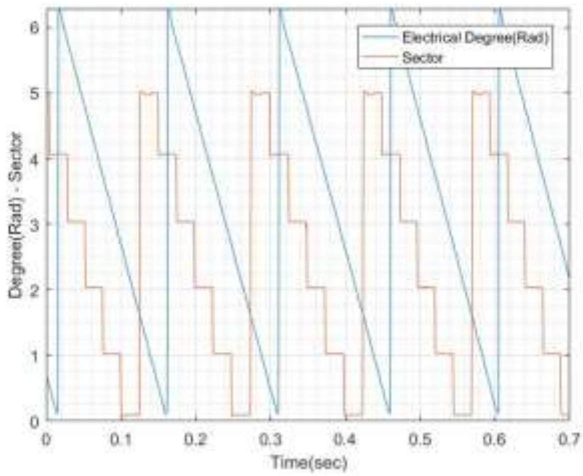

***Figure 13** Space vector sector and space vector when the motor rotates at 100 rpm*

ISSN: 2277-9655
Impact Factor: 4.116
CODEN: IJESS7

IV. CONCLUSION

Cortex M7 core that has been put on the market in recent years has a 216 MHz clock signal and a quite large processing capacity of 462 MIPS. Processor's FPU (floating-point unit) is used for floating numbers, which is used in the field oriented control processes. Thanks to this unit, float numbers can be multiplied much faster. At the Table 1, the comparative results are given which are belonged to the STM32F745VE processor's fast multiplying operation capability.

Table 1 Processors FOC system run times (microsecond)

Processor	PI-Current	SVPWM	Clark	Park	Ipark	ADC	FOC
STM32F745VE (This project results)	1,3	1,96	0,51	3,8	4,14	2,64	14,4
Spartan 3E(FPGA) [24]	0,45	2,31	0,33	0,45	-	0,45	5,4
TMS320f240 [15-16]	5,1	8,3	0,7	2,05	-	7,55	32,6
TMS320C2xx [10]	-	-	5,85		6,83	-	-
Zilog Z8 Encore [23]	26	-	18	28	-	14	-

In this project, software design which has the fastest calculation algorithm used in arm, dsp and microcontroller based sensored PMSM vector applications is executed. As a result, the switching frequency can be increased by reducing the calculation time in every switching cycle.

NOMENCLATURE

i_a, i_b, i_c	Phase currents
I_{sd}	d axis stator current
I_{sq}	q axis stator current
$i_{s\alpha}$	Alpha axis stator current
$i_{s\beta}$	Beta axis stator current
Θ_e	Rotor electrical angle (rad)
V_{ref}	Reference voltage
V_d	Maximum Inverter Voltage
T_s	Pulse width modulation period
V_{qs}	q axes stator voltage
V_{ds}	d axes stator voltage
φ_{ds}	q axes stator flux
φ_{qs}	d axes stator flux
T_e	Motor generated torque
φ_{mag}	Generated flux by magnet
ω	Angular speed of rotor

V. REFERENCES

[1] B. Li, L. Sun, E. Kang, and T. Ding "High Performance and Full Digital AC Position Servo System," Proceedings of the 18th international Conference on electrical machines and systems, ICEMS2005, Nanjing, China, pp. 1869-1872. 27-29st Sept. 2005,

[2] D. Xu, T. Wang, H. Wei. "A digital high performance PMSM servo system based on DSP and FPGA," The 6th IEEE Conference on Industrial Electronics and Applications, 2742-2746, 2011.

[3] C. Naizheng, Y. Guijie, L. Yajing, Z. Pinzhi, "Development of an FPGA-based high-performance servo drive system for PMSM", Proc. 1st Int. Symp. Syst. Contr. Aerosp. Astronaut., pp. 881-886, 2006.

[4] G. Yang; Y. Liu; N. Cui; P. Zhao; "Design and Implementation of a FPGA-Based AC Servo System," - The Sixth World Congress on Intelligent Control and Automation, 2006 WCICA 2006. Volume 2, Page(s): 8145–8149, 21–23 June 2006

[5] Y. Li, S. Zhuang, L. Zhang, "Development of an FPGA-Based Servo Controller for PMSM Drives", Automation and Logistics 2007 IEEE International Conference, pp. 1398, 18–21 Aug. 2007

[6] L. Idkhajine, A. Prata, E. Monmasson, K. Bouallaga and M.-W. Naouar, "System on chip controller for electrical actuator", Proc. ISIE Conf., pp. 2481-2486, 2008-Jul.
[7] Q. Hui and Z. Ya, "Design and Realization of PMSM Vector Control IP Core Based on FPGA", Electrical Machines and Systems, pp. 1325-1328, 2008. ICEMS 2008.
[8] I. Bahri, E. Monmasson, F. Verdier and M. E.-A. Ben Khelifa, "SoPC based current controller for permanent magnet synchronous machines drive", Proceedings of 2010 IEEE International Symposium on Industrial Electronics, ISIE 2010, Bari, Italy, July 2010.
[9] B. Alecsa, M. N. Cirstea and A. Onea, "Simulink modeling and design of an efficient hardware-constrained FPGA-based PMSM speed controller", IEEE Trans. Ind. Inf., vol. 8, no. 3, pp. 554-562, Aug. 2012.
[10] Application note, "Clarke & Park Transforms on the TMS320C2xx ", bpra048, Texas Instrument, http://www.ti.com/lit/an/bpra048/bpra048.pdf
[11] F. Shengwen and Y. Xin, "Design of the low-speed electric vehicle driver based on TMS320F28335", 2015 IEEE 12th International Conference on Electronic Measurement & Instruments, pp. 341-344, July 2015
[12] O. C. Kivanc and S. B. Ozturk, "MATLAB Function Based Approach to FOC of PMSM Drive", IEEE European Modelling Symposium, pp. 96-102, Oct. 2015.
[13] Yu, Shuanghe, Y. Zhenqiang, L. Shuang and Zh. Kai, "Analysis and implementation of digitalized vector control for PMSM with switching control", IEEE. International Conf. ISSCAA, Harbin, China. pp. 912-917, June 2010.
[14] R. Morales-Caporal, O. Sandre-Hernandez, E. Bonilla-Huerta and J. C. Hernandez-Hernandez, "DSP-based space vector modulation for a VSI fed permanent magnet drive", IEEE 9th Int. Conf. Electronics, Robotics and Automotive Mechanics, pp. 261-266, November 2012.
[15] Simon E. "Implementation of a Speed Field Oriented Control of 3-phase PMSM Motor using TMS320F240", Spra588, Texas Instrument Inc., 86p.
[16] Plantic M., "Implementation of Vector Control for PMSM Using the TMS320F240 DSP", Application Report, Spra494, Texas Instrument
[17] Zhenyu Yu, "Space-Vector PWM With TMS320C24x/F24x Using Hardware and Software Determined Switching Patterns", Application Report, Spra524, Texas Instrument
[18] F. Jiang, W. Zhang, W. Liang and X. Liu, "A MC56F8357 Based Permanent Magnet Synchronous Motor (PMSM) Servo System," Proceedings of the Eighth International Conference on Electrical Machines and Systems, ICEMS 2005, vol. 2, pp. 1519-1523, 27-29 Sept. 2005.
[19] X. Xu and G. Hirzinger, "Design of current control of fully integrated surface-mounted permanent magnet synchronous motor drive servo actuator", Proc. IEEE EPE, pp. 9, 2005.
[20] A. M. Vipin, S. George, "Hardware Implementation of Space Vector PWM Control of Permanent Magnet Synchronous Motor", International Conference on Magnetics Machines & Drives (AICERA-2014 iCMMD), 2014.
[21] F. Yusivar, N. Hidayat, R. Gunawan, and A. Halim, "Implementation of field oriented control for permanent magnet synchronous motor", In: IEEE international conference on electrical engineering and computer science. Kuta, pp 359–362, 2014.
[22] M. B. Trivedi and J. J. Patel, "A DSC - Based Field Oriented Control of SPMSM to Mitigate Practical Difficulties with Low Resolution sxIncremental Encoder", International Conference on Computation of Power, Energy, Information and Communication (ICCPEIC), pp. 455–461, 2014
[23] Rabenstein A., "Sensorless Field Oriented Control using an 8-Bit Microcontroller", Infineon Technologies AG, Bodo's Power Systems 2007
[24] Akın Ö. "Asenkron Motor Kontrol Sürücü Sistemleri için Gömülü Sistem Tasarımları ve Gerçeklenmesi", BSc Thesis, Department of Electrical and Electronic Engineering Ege University of Technology, İzmir, Turkey

CITE AN ARTICLE

Altıntaş, M. (n.d.). SENSORED VECTOR CONTROL THREE PHASE MOTOR DRIVER DESIGN BASED ON CORTEX M7 ARM . *INTERNATIONAL JOURNAL OF ENGINEERING SCIENCES & RESEARCH TECHNOLOGY*, *6*(12), 285-294.